Regular Article

INORGANIC CHEMISTRY RESEARCH
Published by the
Iranian Chemical Society
www.inorgchemres.org
info@inorgchemres.org

Inorg. Chem. Res., Vol. 2, No. 1, 6-15, June 2019
DOI: 10.22036/icr.2018.102753.1040

A New Mixture of Nano-structure of Potassium-incorporated Hydroxyapatite/β-tricalcium Phosphate/calcium Pyrophosphate

M. Chahkandi[a,*] and B. Chahkandi[b]

[a]*Department of Chemistry, Hakim Sabzevari University, Sabzevar 96179-76487, Iran*
[b]*Department of Chemistry, Shahrood Branch, Islamic Azad University, Shahrood, Iran*

(Received 30 October 2017, Accepted 23 April 2019)

The new triphasic potassium-substituted hydroxyapatite (KHAP), β-tricalcium phosphate (β-TCP), and calcium pyrophosphate (CPP) proportions using easy sol-gel method were synthesized. The prepared powders were characterized by X-ray diffraction (XRD), Fourier transform infrared (FTIR), Differential thermal behavior (DTA) analysis, Energy Dispersive X-ray Analysis (EDXA) and Brunauer-Emmett-Teller (BET). In addition, the size of nano particle and micro-strain of the synthesized samples using Williamson-Hall (W-H) plots and transmission electron microscopy (TEM) were measured. The (K + Ca)/(P + C) molar ratio in the KHAP samples was around to be 1.67. Actually, the incorporation of potassium in the calcium deficient apatites was accompanied by the formation of mentioned triphasic mixture ceramics, upon calcination from 400 to 600 °C. However, increasing of the firing temperature to 700 °C resulted in growth of the HAP content as the dominant phase. The XRD peaks of these prepared nano-structures show same pattern with pure HAP phase with hexagonal structure and $P6_3/m$ space group. Moreover, the evaluated particle size of synthesized samples by W-H and TEM methods are in good agreement as 25-95 nm. Surface area of calcined KHAP samples at 400 to 700 °C were found as 127.83, 48.39, 12.91 and 5.32 $m^2 g^{-1}$, respectively.

Keywords: Potassium-substituted hydroxyapatite/β-TCP/CPP, Nano-particles, Sol-gel

INTRODUCTION

The well-known Ca-P ceramic; hydroxyapatite (HAP, $Ca_5(PO_4)_3(OH)$); is the inorganic component of human hard tissues like bone, dentine, and enamel [1]. Since, HAP shows good biocompatibility, inductivity for bone ingrowth, low-cost preparation, non-toxicity, and high adsorptive capabilities, it possess interesting bio-properties such as biomedical applications [2-5], drug delivery [6], antitumor [7], cell proliferation [8], heavy metal and organic pollutants capture [9], and photocatalysis [10]. The various approaches have been applied for preparation of HAP particles resulting in difference of shapes and size such as solid-state conditions, wet methods (co-precipitation, sol-gel, hydrothermal, biomimetic method, microemulsion synthesis, *etc.*) and many others [11-15]. During the last decade, the working up about the cation-doped HAPs has opened up a new arena of various application fields like biomedical, dentistry, and purification systems. Therefore, in the recent years, the elemental substitution in the apatite structure has been the field of special interest. The substitution or doping of calcium ions, phosphate groups or hydroxyl groups in HAP is possible [16]. Copper substituted HAP about the uranium [17], Ag-doped HAP about the Congo Red dye (CR) [18], HAP loaded with strontium about the soybean oil [19], and silicon doped HAP for copper [20] adsorption can be mentioned. However, a few researches have been done on the substitution of potassium in HAP which show the incorporation in the apatite lattice without significant changes in the structural parameters [21]. Potassium has capability in the regulation of biochemical and apatite

*Corresponding author. E-mail: m.chahkandi@hsu.ac.ir

mineral nucleation processes [22,23]. K-substituted HAP should be a better material comparing the individual HAP or β-tri calcium phosphate (β-TCP) [21]. Till now, there is no scientific report on the processing of triphasic mixtures of potassium substituted-HAP (KHAP), β-TCP, and calcium pyrophosphate (CPP) components. It can be mentioned, the aim of this work is an effort for preparation of this new triphasic ceramic mixture through sol-gel method.

Herein, sol-gel technique because of simplicity, homogeneity of product, and capability to make nanoparticles was applied for preparation of new triphasic Ca-P compound. In followings, the sample is characterized by powder XRD, FTIR, DTA and EDXA. Moreover, the particle size is estimated by XRD and TEM (see part 3.2.). Also, the effect of firing temperature on the sample purity, particle size, and micro-strain is investigated. The obtained results of nano-particle size of KHAP from W-H and TEM analyses show good consistency.

MATERIALS AND METHODS

KHAP Sol-gel Synthesis and Physical Measurement

First of all, triethyl phosphate ($(C_2H_5O)_3PO$, TEP, Fluka) was hydrolyzed for 24 h at R.T. along with the vigorous stirring. Then, the aqueous solution of 3 M $Ca(NO_3)_2{\cdot}4H_2O$ (Merck) and 3 M KNO_3 (28 w/w% K) were added slowly to 4 M hydrolyzed TEP ((Ca + K)/P = 1.67) at a rate of 6 ml min^{-1}. Next, the respected sol solution was vigorously stimed for 60 min at 80 °C. Finally, the obtained clear solution was aged for 48 h at R.T. In order to better follow the progress of the sol-gel process, the *p*H values of the sample solutions before and during aging were recorded. After that, the aged sol was dried at 100 °C until a white dried gel was obtained. The as-prepared gel structure was analyzed using differential thermal analysis (DTA, Netzsch, Germany) and IR spectroscopy (Buck 500, KBr) in the range of 500-4000 cm^{-1}. The dried gel was ground into fine powder and then calcined at different firing temperatures (400, 500, 600 and 700 °C) for 2 h at a constant heat rate of 2 °C min^{-1}. Phase identification and characterization of the calcined gel of KHAP was performed using the X-ray diffractometer (XRD, Philips, X´pert Pro, Cu Kα, Ni Kβ) at a scanning speed of 1° 2θ min^{-1} from 20 to 55° and IR spectroscopy (Buck 500, KBr) in the range of 500-4000 cm^{-1}. Elemental analyses for the presence of Ca, K, and P were made using Energy Dispersive X-ray Analysis (EDXA) (Philips PW2400 X-Ray Fluorescence Spectrometer); W/W%: K 28.7%, Ca 7.98%, P 11.7%, C 6.70%. The Surface area of synthesized KHAP samples was measured by physical adsorption of N_2 using the Brunauer-Emmett-Teller (BET, Quantachrome Instruments, USA) method.

Particle Size Determination

Particle size and micro-strain of KHAP powders with the aid of Scherrer and Williamson-Hall equations [24,25] were calculated. Also, particle size distribution was determined by TEM observations. TEM (Leo 912 AB-Germany) was equipped with a thermionic gun and was operated at 120 kV. TEM samples were prepared as follows: the KHAP powders were ultrasonically dispersed for 2 h in absolute ethanol and afterward deposited on a carbonated copper grid.

RESULTS AND DISCUSSION

XRD Analysis

Figure 1 shows the XRD patterns of calcined KHAP samples at the range of 400-700 °C. All sample powders have indicated the apatite phase formation with different peak intensity and width. There are the intense peaks of HAP, β-TCP, CPP and also impurity phase of CaO which match the ICDD standards (JCPDS). The indices of HAP ((002), (210), and (211)), β-TCP ((217) at 30.7°), and CPP ((100) at 26.7°)) confirm the hexagonal, rhombohedral, and monoclinic systems, respectively. Raising of firing temperature increases the crystallinity and transformation of Ca-P phases to HAP structure. In fact, manipulation of aging and thermal treatment steps of sol-gel process can improve the purity of final product due to the betterment of polymerization reaction between Ca, K and P precursors [12]. Therefore, we used TEP hydrolysis (Eq. (1)) as an advantage comparing to the other works [26] that provides more completed of polymerization reaction and increasing of HAP phase (Eq. (2)).

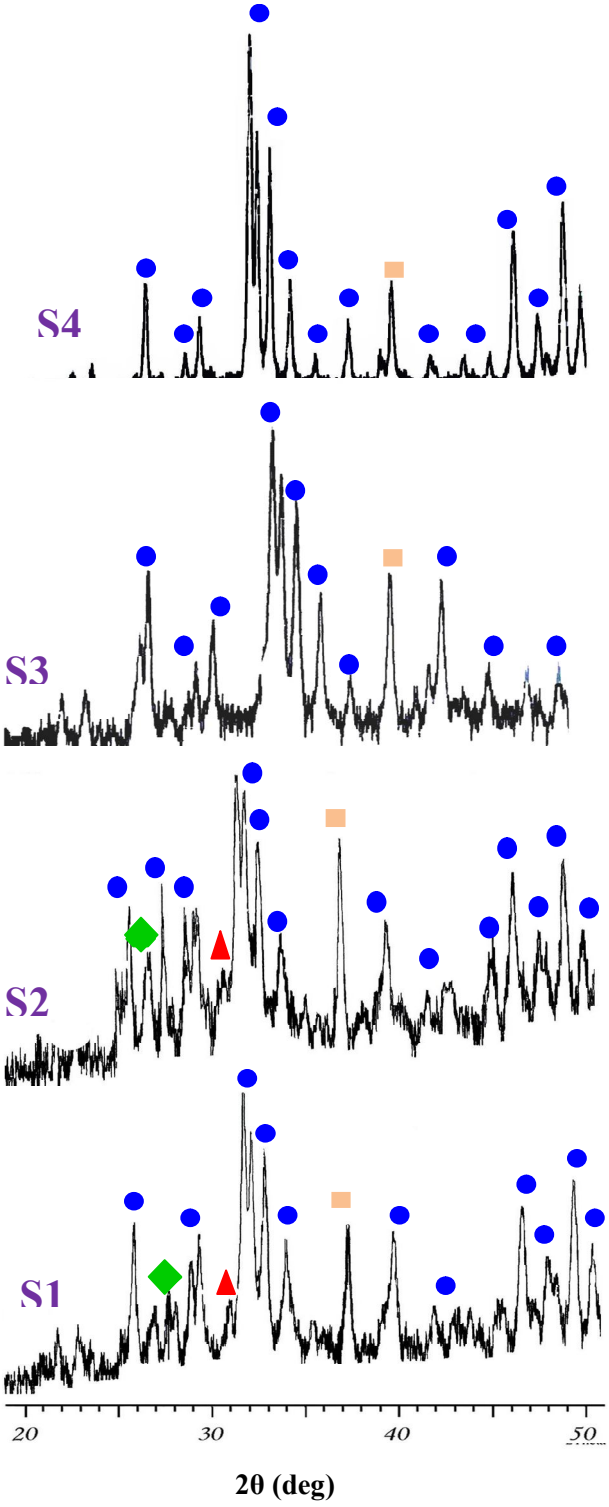

Fig. 1. X-ray diffraction patterns of KHAP samples (S1-S4) calcined at 400, 500, 600 and 700 °C, respectively, shown: (●) HAP; (■) CaO; (▲) β-TCP; and (♦) $Ca_2P_2O_7$.

$$OP(OEt)_3 + H_2O \rightarrow OP(OEt)_{3-x}(OH)_x + xC_2H_5OH \quad (1)$$

$$OP(OEt)_{3-x}(OH)_x + Ca^{2+} + K^+ + NO_3^- \rightarrow (NO_3)^-(OH)\text{-}Ca\text{-}O\text{-}K\text{-}PO(OEt)_{3-x} + H^+ + C_2H_5OH + H_2O \quad (2)$$

The diffraction patterns indicate that potassium can be incorporated in the crystal structure of apatite without significant changes in the apatite phase behavior in spite of small discrepancies of lattice parameters [21]. However, XRD patterns of calcined KHAP samples resemble HAP phase even though having Ca/P ratio with greater or less than the stoichiometric molar ratio of 1.67 for pure HAP [21(a)]. It should be noted that the replacement of Ca^{2+} by K^+ monovalent causes to the charge imbalance that can be neutralized by the substitution of PO_4^{3-} by CO_3^{2-} or creating supplementary vacancies [27].

FTIR Spectra

The surface functional groups of KHAP nano-particles can be followed by FTIR spectrum (Fig. 2). The spectra of as-prepared and calcined powders (Fig. 2 down and up, respectively) support the apatite phase formation that the functional vibrational modes observed at: (i) For as-prepared gel the bands at 1232 and 1370 cm^{-1} indicate the stertching mode of OEt due to the incompleat hydrolysis of TEP (Eq. (1)). The vibration bands at 746, 952 and 1441 cm^{-1} were assigned to NO_3^- because of very hygroscopic character of reminding $Ca(NO_3)_2$ precursor in the gel. The broaden band at 3200-3700 cm^{-1} attributed to stertching mode of -OH and its band of bending mode appeared at 3555 cm^{-1}. Moreover, the located bands at 817, 1054 and 2977 cm^{-1} assigned to PO_4^{3-} confirm the HAP presece in the as-prepared gel [28]. The presence of carbonate ion can be followed by observation the band at 1630 cm^{-1} related to stretching mode of C=O in CO_3^{2-} group. The vibratonal spectrum of sintered KHAP at 400 °C (Fig. 2 up side) includes the bands at 565, 1044, 1420-1460 and 3433 cm^{-1} could be assigned to modes of phosphate, carbonate, and O-H functional groups, respectively. Also, the appearance of band at 720 cm^{-1} for S1 and S2 confirms the presence of pyrophosphates ($P_2O_7^{4-}$) (see Fig. 2).

It should be highlighted that the observed results show good consistency with the literature [12,15,29].

DTA

The DTA curve of the as-prepared gel (Fig. 3) shows two major peaks: a weak exothermic one at ~400 ºC and the strong endothermic one at 560 ºC. It can be disscused that the peak at 400 ºC could be attributed to transformation of amorphous apatite phase to the crystallite one, and the endothermic one at 560 ºC is corresponded to the transformation of calcium phosphate (Ca-P) phase to the crystalline KHAP phase (see Eq. (3)).

$$1/2Ca_2P_2O_7 + Ca_3(PO_4)_2 + Ca(NO_3)_2 + CaCO_3 + 1/2H_2O \rightarrow Ca_5(PO_4)_3(OH) + CaO + 2NO_2 + CO_2 + 1/2O_2 \quad (3)$$

In addition, the observation of an intense exothermic peak at 210 °C can be assigned to extrude of the nitrogenous gases. It should be concluded that increasing the calcination temperature over 400 °C promotes the transformation of Ca-P secondary phases to the apatite one.

Nanostructural Examination

The low calcination temperatures employed in sol-gel method prepared the small particles of gells having high surface energy that makes highly agglomerated crystal with significant prososity. FESEM images confirm this cliam with showing the significant agglomeration of particles (see Fig. 4; because of resemblance just the image of S1 has been shown).

The EDXA elemental analysis has determined the (Ca + K)/(P + C) molar ratio of 1.67 resulting the proposed $(Ca_{2.94}K_{2.06})(PO4)_{0.94}(CO3)_{2.06}(OH)_1$ formula that confirmed the synthesize of carbonate KHAP (see Fig. 2). In order to measurement of particle size of samples two complementary methods, TEM and XRD, have been used. TEM as a most current direct method, provides real picture including the homogeneity impression of particles. Limiting of considering the typically several hundreds of particles known as its main disadvantage. Nevertheless, XRD as an indirect method provides the simple estimating approach of particle size using the so-called Scherrer formula (see Eq.

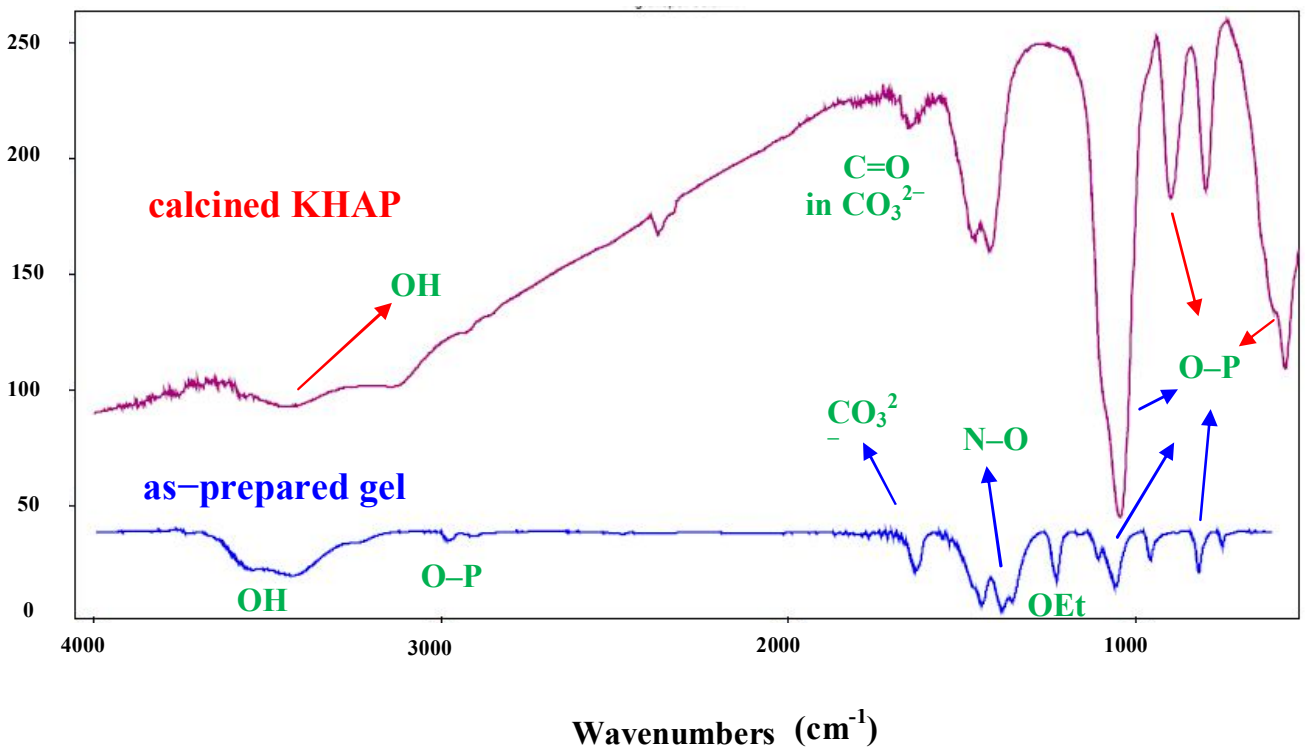

Fig. 2. FTIR of powder samples of KHAP calcined at 400 °C (up) and as-prepared gel (down).

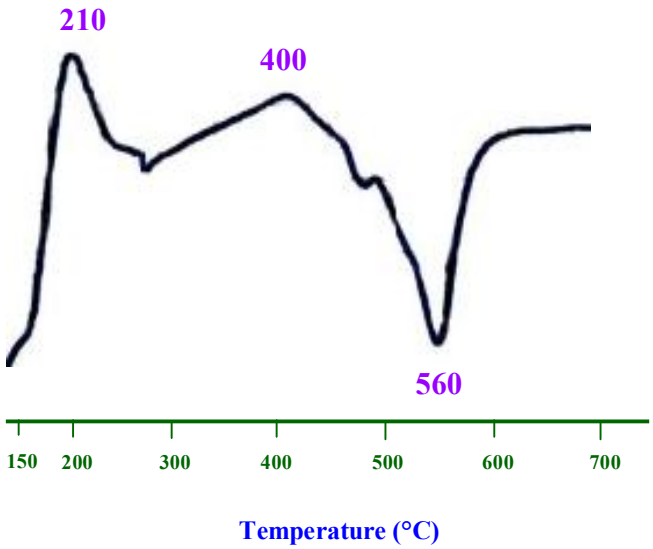

Fig. 3. DTA curve of the as-prepared gel of KHAP.

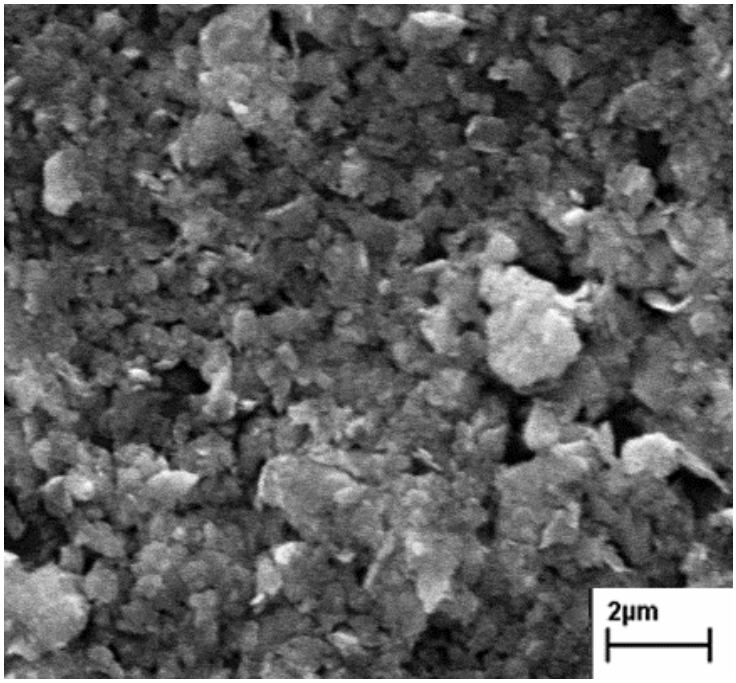

Fig. 4. FESEM of sample S1 calcined at 400 ºC shows highly agglomeration.

(4)) [12,15,30]:

$$D = K\lambda/[W\cos\theta] \quad (4)$$

where K is a constant value of 0.9, λ is the Cu K*α* radiation (0.1544 nm), W is the full width at half-maximum, and θ is the diffraction angle (deg).

Figure 5 depictes the TEM images of S1-S4 KHAP powders. It is obvious that, raising the calcination temperature from 400 up to 700 ºC makes the growthing of particles size. The measured domain particle size of S1, S2, S3, and S4 range from 20-30, 34-45, 53-67 and 75-115 nm, having the mean size values as 24, 39, 60 and 95 nm, respectively. It should be noted that the TEM data confirm the exported results of XRD patterns in a good shape (*vide infra*).

The peak width of the XRD pattern indicates the contribution of crystallite size, micro-strain ϵ_s, and the instrument effect [30]. Stokes and Wilson expressed influence of ϵ_s in line broadening (Eq. (5)) [31].

$$W_\epsilon = 4\epsilon_s \tan(\theta) \quad (5)$$

However, for deconvolution of size and instrumental effect on XRD peak width the more accurate Williamson-Hall (W-H) method using the *Gauss* approximation (Eq. (6)) was used (For more information see the literature [12,15,25]).

$$(W\cos\theta)^2 = (K\lambda/D)^2 + 16\epsilon_s^2 \sin^2\theta \quad (6)$$

The size of crystallite particle (D) of S1-S4 and their ϵ_s can extracted from plot of respected W-H curve of $(W\cos\theta)^2$ *vs.* $\sin^2\theta$ for (002), (210), (211), (300) and (310) reflections (see Fig. 5). The measured results have been shown in Table 1. According to the above discussion increasing of the firing temperature is resulted in improving of the particles crystallinity, sharpening of XRD peak width, and increasing of the particle size.

BET

The N_2 adsorption-desorption isotherm of KHAP samples can be used for measuring the specific surface area (see Fig. 6.). The curves show the type *IV* isotherm including H3 type of hysteresis loop, confirming the

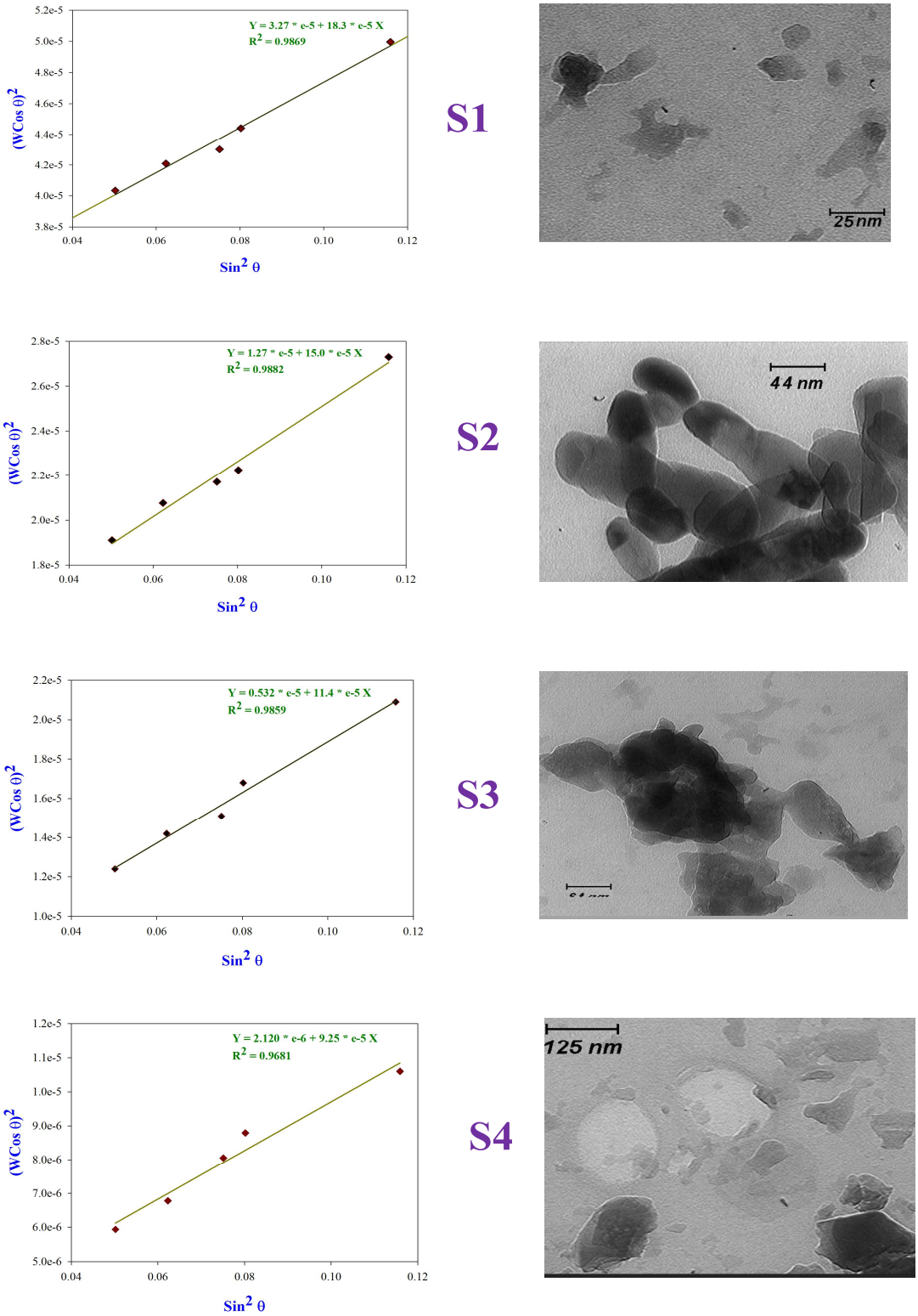

Fig. 5. Deconvolution of strain and size effects of S1-S4 KHAP samples using Gauss approximation, by W-H plots (left side) and their TEM images (right side).

Table 1. Comparison of XRD Results Using Gauss Correction for Instrumental Broadening

Sample	Firing Temp. (°C)	Williamson-Hall	
		D (nm)	Micro-strain (°)
S1	400	24.3	3.38E-3
S2	500	39.0	3.06E-3
S3	600	60.3	2.62E-3
S4	700	95.4	2.40E-3

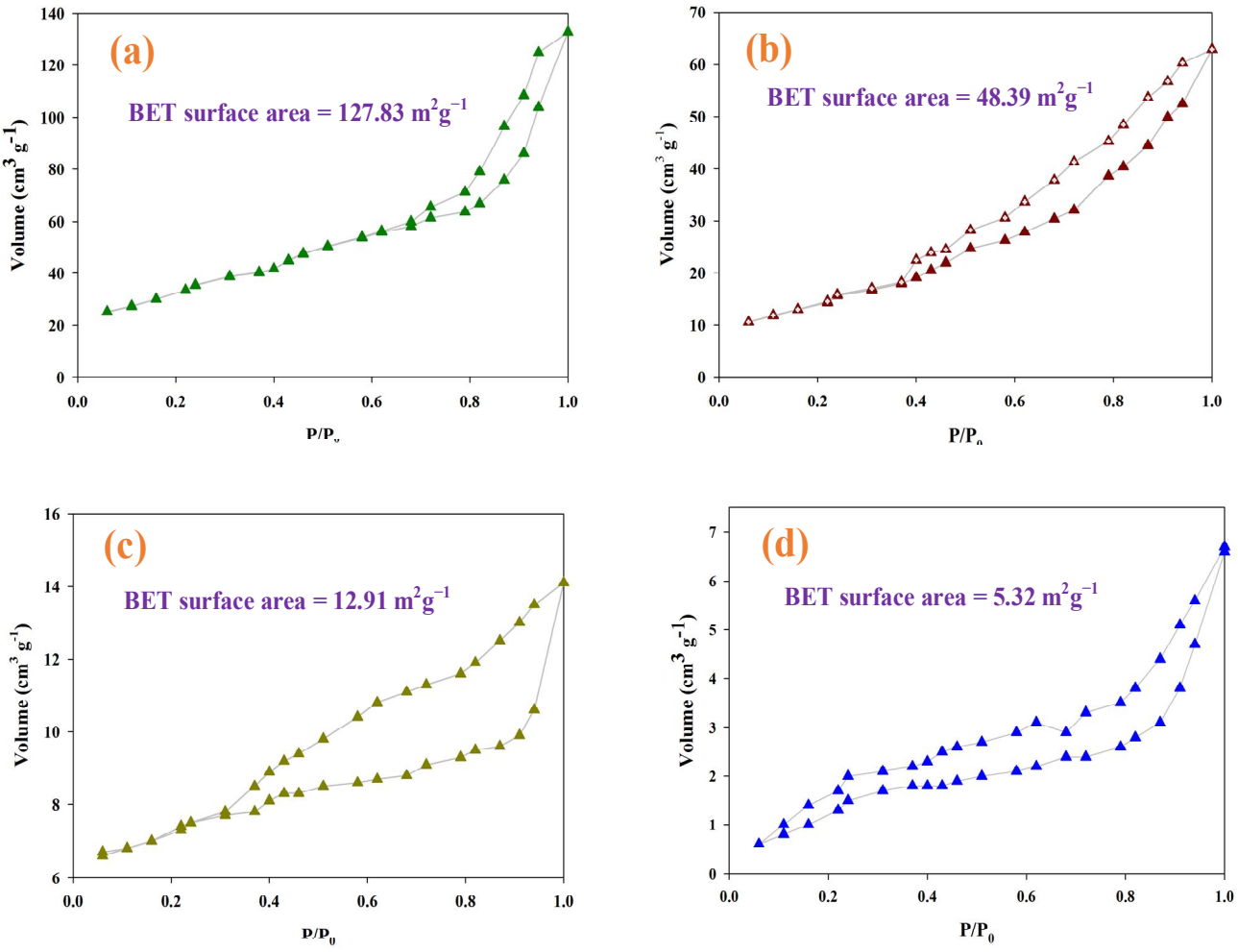

Fig. 6. N_2 adsorption-desorption isotherms for samples of KHAP nanoparticles (a) S1, (b) S2, (c) S3 and (d) S4.

presence of mesopores and micropores [32]. Surface area specifies the interface of a solid that interacts with its surroundings. Actually, decreasing of particle size results in increasing of surface area per unit volume or mass. Determined surface area confirms this claim as the BET surface area for S1 to S4 samples decreased from 127.83 to 5.32 $m^2 g^{-1}$ as their particle size increased from 24.3 to 95.4 nm (see Figs. 5 and 6 and Table 1).

CONCLUSIONS

Herein, the easy sol-gel method with low temperature condition applied for synthesize the nano-strucure of new mixture of potassium substituted HAP/β-TCP/CPP that in following using XRD, FTIR, EDXA and TEM analyses, the structure and particle size evaluation studied. EDXA results propose $(Ca_{2.94}K_{2.06})(PO4)_{0.94}(CO3)_{2.06}(OH)_1$ formula for the prepared KHAP compound calcined at 700 °C. DTA and XRD results of prepared KHAP powders showed that the HAP phase formation has begun at the low temperature of 400 ºC. This is because of high surface energy of small size particles of as-prepared gel. The improved Scherrer's equation with considering the W-H method and TEM images measured the mean particle size as 25-95 nm for S1−S4 calcined at 400, 500, 600, and 700 °C, respectively. Measuring the amount of N_2 physisorbed to KHAP samples surface shows decreasing of particle size leads to increasing of specific surface area. In addition, increasing the firing temperature leads to remarkable improving of the crystallinity, increasment of crystallite size, and reduction of micro-strain of mosaic blocks.

ACKNOWLEDGMENTS

MCH gratefully acknowledges the financial support by the Hakim Sabzevari University, Sabzevar, IRAN.

REFERENCES

[1] P. Tschoppe, D.L. Zandim, P. Martus, A.M. Kielbassa, J. Dent. 39 (2011) 430.

[2] D. Eichert, C. Drouet, H. Sfihi, C. Rey, C. Combes, Nanocrystalline Apatite-based Biomaterials: Synthesis, Processing and Characterization, in: J.B. Kendall (Ed.), Biomaterials Research Advances, Nova Science Publishers, New York, 2007, pp. 93-143.

[3] Y. Cai, R. Tang, J. Mater. Chem. 18 (2008) 3775.

[4] S.V. Dorozhkin, Biomaterials 31 (2010) 1465.

[5] G. Ciobanu, S. Ilisei, C. Luca, Mater. Sci. Eng. C Mater. Biol. Appl. 35 (2014) 36.

[6] G.D. Venkatasubbu, S. Ramasamy, V. Ramakrishnan, J. Kumar, Biotech. 1 (2011) 173.

[7] G. Li, L. Ye, J. Pan, M. Long, Z. Zhao, H. Yang, J. Tian, Y. Wen, S. Dong, J. Guan, B. Luo, Liver Int. 32 (2012) 998.

[8] F. Zhang, B. Ma, X. Jiang, Y. Ji, Powder Technol. 302 (2016) 207.

[9] A. Amiri, M. Chahkandi, A. Targhoo, Anal. Chim. Acta 950 (2017) 64.

[10] G. Bharath, N. Ponpandian, RSC Adv. 5 (2015) 84685.

[11] Y. Zhang, J. Lu, J. Nanopart. Res. 9 (2007) 589.

[12] H. Eshtiagh-Hosseini, M.R. Housaindokht, M. Chahkandi, Mater. Chem. and Phys. 106 (2007) 310.

[13] G. Ciobanu, G. Carja, O. Ciobanu, Surf. Coat. Tech. 202 (2008) 2467.

[14] G. Ciobanu, S. Ilisei, C. Luca, G. Carja, O. Ciobanu, Prog. Org. Coat. 74 (2012) 648.

[15] M. Chahkandi, M. Mirzaei, J. Iran Chem. Soc. 14 (2017) 567.

[16] Y. Tang, H.F. Chappell, M.T. Dove, R.J. Reeder, Y.J. Lee, J. Biomater. 30 (2009) 2864.

[17] G. Liu, J. Talley, C. Na, S. Larson, L. Wolfe, Environ. Sci. Technol. 44 (2010) 1366.

[18] C. Srilakshmi, R. Saraf, Microporous and Mesoporous Mater. 219 (2016) 134.

[19] C. Wei, H. Zhiliang, L. Yu, H. Qianjum, Catal. Commun. 9 (2008) 516.

[20] E.S. Bogya, R. Barabas, A. Savdari, V. Dejeu, I. Baldea, Chem. Pap. 63 (2009) 568.

[21] a) S. Kannan, J.M.G. Ventura, J.M.F. Ferreira, Ceramics International 33 (2007) 1489; b) E.G. Nordstrom, K.H. Karlsson, Biomed. Mater. Eng. 2 (1992) 185; c) H. El. Feki, T. Naddari, J.M. Savariault, A. Ben Salah, Solid State Sci. 2 (2000) 725; d) A. Smahi, A. Solhy, H. El Badaoui, A. Amoukal, A. Tikad, M. Maizi, S. Sebti, Appl. Catal. A: Gen. 250 (2003) 151.

[22] C.H. Suelter, Science 168 (1970) 789.
[23] H.J. Hohling, H. Mishima, Y. Kozawa, T. Daimon, R.H. Barckhaus, K.D. Richter, Scanning Microsc. Int. 5 (1991) 247.
[24] G.K. Williamson, W.H. Hall, Acta Metall. 1 (1953) 22.
[25] A. Weibel, R. Bouchet, F. Boulc'h, P. Knauth, Chem. Mater. 17 (2005) 2378.
[26] a) K. Cheng, W. Weng, G. Han, P. Du, G. Shen, J. Yang, J.M.F. Ferreira, Mater. Chem. Phys. 78 (2003) 767; b) Cheng, W. Weng, G. Han, P. Du, G. Shen, J. Yang, J.M.F. Ferreira, Mater. Res. Bull. 38 (2003) 89.
[27] H. El. Feki, A. Ben Salah, A. Daoud, A. Lamure, C. Lacabanne, J. Phys. Condens. Matter 12 (2000) 8331.
[28] L.-Y. Huang, K.-W. Xu, J. Lu, J. Mater. Sci. Mater. Med. 11 (2000) 667.
[29] L. Cui, Y. Wang, L. Hu, L. Gao, B. Du, Q. Wei, RSC Adv. 5 (2015) 9759.
[30] H. Borchert, E.V. Shevchenko, A. Robert, I. Mekis, A. Kornowski, G. Grübel, H. Weller, Langmuir. 21 (2005) 1931.
[31] E. Tkalcec, M. Sauer, R. Nonninger, H. Schmidt, J. Mater. Sci. 36 (2001) 5253.
[32] K.S.W. Sing, D.H. Everett, R.A.W. Haul, L. Moscou, R.A. Pierotti, J. RouqueroL, T. Siemieniewska, Pure Appl. Chem. 57 (1985) 603.